Available online at www.eccomasproceedia.org
Eccomas Proceedia UNCECOMP (2023) 684-694

ECCOMAS
Proceedia

UNCECOMP 2023
5th ECCOMAS Thematic Conference on
Uncertainty Quantification in Computational Science and Engineering
M. Papadrakakis, V. Papadopoulos, G. Stefanou (eds.)
Athens, Greece, 12-14 June 2023

EXPERIMENTAL INVESTIGATION OF THE UNCERTAINTY OF DISORDERED FIBER-REINFORCED INJECTION-MOLDED COMPONENTS

Benedikt Rohrmüller[1], Franziska Kneisel[1], Jörg Hohe[1], and Carla Beckmann[1]

[1] Fraunhofer Institute for Mechanics of Materials IWM
Wöhlerstr. 11, 79108 Freiburg, Germany
e-mail: benedikt.rohrmueller@iwm.fraunhofer.de

Abstract

Short fiber-reinforced composites manufactured by injection molding exhibit an alignment of the fibers superimposed by a manufacturing process induced scatter. As a result, the components possess a scatter in their mechanical properties due to the local scatter in fiber length, fiber orientation and fiber volume content. In this paper, we investigate the scatter of mechanical properties and fiber orientation of a glass fiber-reinforced phenolic resin with a fiber mass content of 37.5 wt% manufactured by a thermoset injection molding process [1]. Rectangular plates of 2 and 3 mm thickness and a size of 190 x 480 mm² were manufactured.
The objective is to investigate the local variation of mechanical properties (Young's modulus, tensile strength and fracture strain) and fiber orientation and to evaluate the data statistically. Tensile tests are performed on miniature specimens of 36 mm length, 2 mm thickness and 2 mm width tested in 0° and 90° direction. The local mechanical properties are correlated with the local fiber orientation evaluated on in-plane micrographs taken on every specimen. On the 3 mm plates, tensile tests on specimens with shortened ISO dimensions are performed. The strain is evaluated globally and locally by digital image correlation (DIC).
The investigated material shows fiber alignment in flow direction with the sprue positioned in the middle of the plates. The fiber alignment is superimposed by a large local process induced variation of the fiber orientation.

Keywords: Short fiber-reinforced polymers, Characterization, Uncertainty Quantification, Multiscale Analysis.

ISSN:2623-3339
Peer-review under responsibility of the organizing committee of UNCECOMP 2023.
doi: 10.7712/120223.10367.19897

1 INTRODUCTION

Short fiber-reinforced polymers are used in lightweight construction due to their low specific density. Fiber-reinforced polymers produced by the thermoset injection molding process can achieve the material properties of aluminum, while requiring less energy in production [2]. However, short fiber composites have a disordered and process-dependent microstructure. This leads to a local scatter of fiber orientation, fiber length and fiber volume content, which results in a scatter in material behavior. In order to better exploit the lightweight potential, the uncertainty of the material behavior must be taken into account in the design process. The consideration of the uncertainty can be done by probabilistic multiscale simulations along the process chain, in which case uncertainty is considered in both, process simulations and structural mechanics simulations. To investigate the material uncertainty, specimens can be taken from the same positions of different components, or many different samples can be taken from one component.

In the thermoset injection molding process, fiber plastic mixtures are plastified in a screw extruder and injected under high pressure into a cavity where they solidify. The fibers change their orientation due to the flow. Different orientation layers form over the component thickness. Even though the layers have preferred directions, scattering and a disordered reinforcing structure still exist [3]. The thermoset injection molding process delivers high component quality via holding pressure and temperature control. Nevertheless, the material and the process are exposed to varying influences (storage time, temperature, humidity, etc.), which cause scatter even in a stable process [4]. In [5], for example, scattering of the material temperature at the inlet to the cavity was observed. In addition, scattering of the fiber length occurs because the fibers break during the process, which also affects the component properties [6]. In [1], a fiber volume dependence of the fiber length was also observed. With a higher fiber volume content, the fibers are shorter on average.

We investigate experimentally the scatter of the mechanical properties on 2 and 3 mm thick plates for one fiber mass content for a short-glass fiber-reinforced phenolic resin. A large number of small specimens taken from two 2 mm thick plates is tested to get an information on the scatter of the mechanical properties in a plate. The evaluation of micrographs of the specimen heads enables the correlation of the mechanical properties with the fiber orientation. Larger ISO specimens taken always from the same position of different plates are tested to investigate the scatter of the mechanical properties between different plates.

2 EXPERIMENTAL INVESTIGATION

2.1 Material

The investigated material is a glass fiber-reinforced phenolic resin with a fiber mass content of 37.5 wt% manufactured by a thermoset injection molding process [1]. The glass fibers possess a diameter of 13 µm and an initial length of 4 mm. After manufacturing the fiber length has a scatter with a mean value of 378 µm [1]. The manufacturing was done at Fraunhofer ICT in Pfinztal, Germany. Rectangular plates of size 480 x 190 mm² with a central sprue and 2 and 3 mm thickness were manufactured.

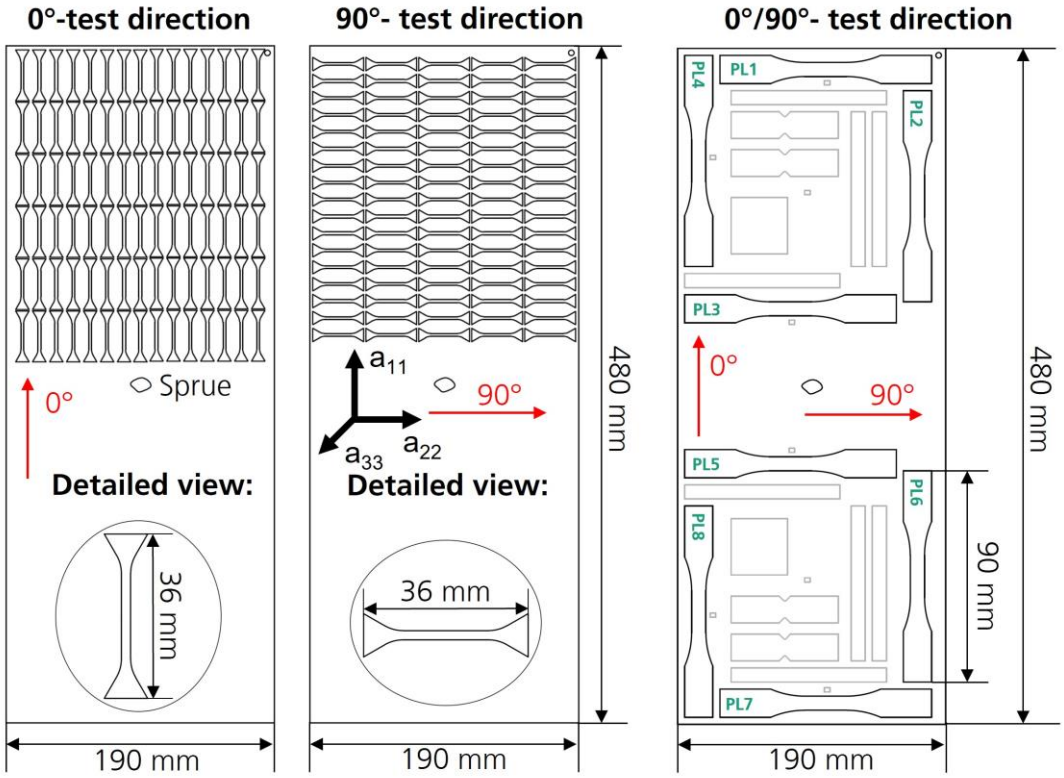

Figure 1: Tensile specimens.

2.2 Experiments and evaluation

Quasi-static tensile tests are performed on specimens of two different scales with cross-sections of 2 x 2 mm² and 3 x 10 mm². The specimen plan is shown in Fig. 1. Miniature specimens with a length of 36 mm are taken from two 2 mm thick plates (see Fig. 1 left and middle). 90 miniature specimens were taken in 0°-direction and 85 in 90°. To investigate the scatter between different plates, shortened ISO size tensile specimens after DIN EN ISO 527-4 [7] with a width of 10 mm are taken from 3 mm thick plates. The specimen plan is shown in Fig. 1 right. Four specimens in 0° and four in 90° are placed on one plate. Two 90° specimens are placed sprue near and two specimens sprue far. In addition, shear and compression specimens are extracted from the 3 mm thick plates, the results of which are not shown here. Here, results of 56 tensile tests on ISO specimens (28 each in 0° and 90° direction) will be shown, which are taken from seven different plates. All specimens were cut out by water-jet cutting.

An electro mechanical testing machine is used for the tensile tests. All specimens are tested until fracture. The miniature specimens are tested with a velocity of 1 mm/min. The strain on the miniature specimens is measured by an extensometer with an initial length of $l_0 = 10$ mm. The ISO specimens are (except for some specimens at the beginning) tested with a velocity of 4 mm/min. The strain on the ISO specimens is measured optically. A speckle pattern is applied on one specimen side. The local and global strain is evaluated afterwards by digital image correlation in the software GOM Aramis. All specimens are evaluated with respect to their engineering stress and engineering strain. The engineering stress is defined by

$$\sigma_{\text{eng}} = F/A_0 \tag{1}$$

with the force F and the initial cross-section A_0. The engineering strain is defined by

$$\varepsilon_{eng} = l/l_0 \tag{2}$$

with the actual length l and the initial length l_0. The Young's modulus E, the tensile strength R_m and the fracture strain A are evaluated for every specimen.

2.3 Determination of fiber orientation tensor

The fiber orientation is determined on one specimen head of each tested dogbone shaped miniature specimen. The lower specimen head of each tested specimen in Fig. 1 was taken from the 0° specimens and the left head from the 90° specimens. The specimen heads are in-plane ground and polished at a depth of 100-200 µm from the surface. The fiber orientation tensor (FOT) of second order after [8], here termed a_{ij}, with i,j={1,2,3} is determined from microscopic images of size 1.3 x 1.6 mm². The FOT is evaluated with respect to the coordinate system in Fig. 1 middle. The microscopic images are selected as representative of the whole specimen head. The segmentation of images and the evaluation of the FOT is done in Matlab. Fibers that are too close together to be detected automatically are separated manually. Due to the large local scatter of the fiber distribution, the determined fiber orientation possesses a large scatter.

3 RESULTS

The tensile test results of the two specimen sizes are shown in separate sections. At the end, the mechanical characteristics (Young's modulus, tensile strength and fracture strain) of the two specimen sizes are compared with respect to their cumulative distribution functions.

3.1 Miniature specimens

The stress-strain curves of the miniature specimens are shown in Fig. 2 for 0° and 90°. All tensile tests show a brittle fracture behavior with a fracture strain slightly above 1%. The specimens show no necking. The tensile strength for 0° specimens is higher than for the 90° specimens.

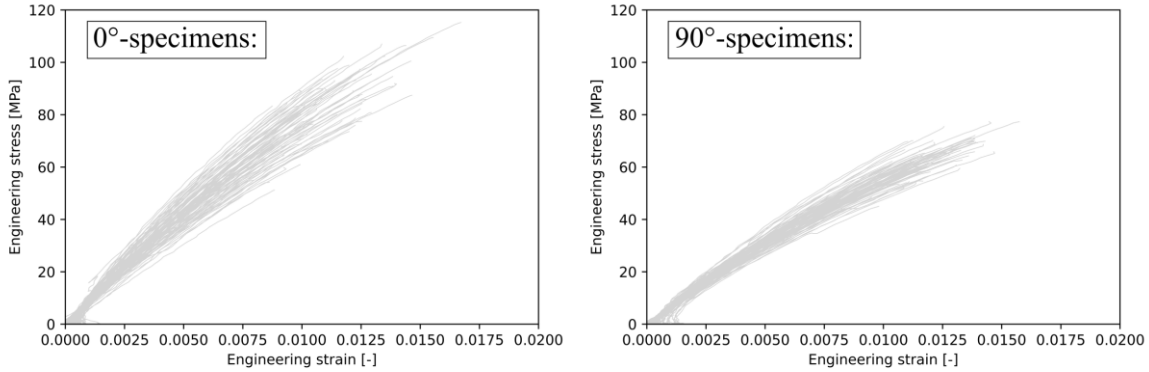

Figure 2: Stress-strain curves of miniature specimens in 0° and 90°.

The mechanical properties of the miniature specimens are shown mapped on the plates in Fig. 3. Each colored rectangle corresponds to the position of a specimen. In this way, the scatter of the mechanical properties can be compared with the positions of the specimens. The Young's modulus and the tensile strength are both higher for the 0° specimens. Next to the

sprue, in the bottom row, the Young's modulus and the tensile strength are both lower for the 0° specimens. For the 90° specimens, they are slightly higher in the bottom rows. The tensile strength of 0° specimens is higher in the middle of the half plate. The fracture strain values do not show a clear direction dependent behavior. All values show a scatter over the plates.

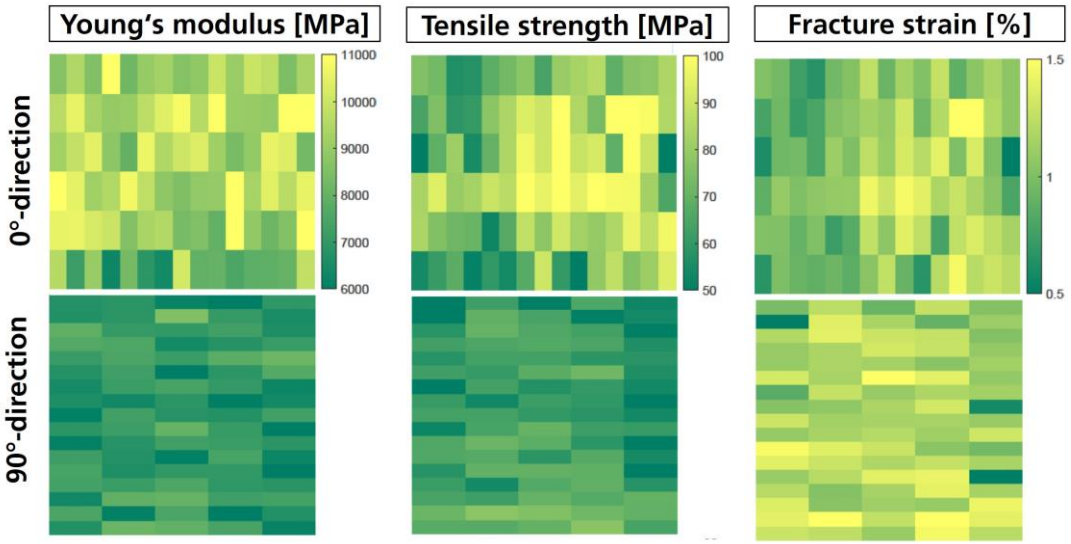

Figure 3: Mechanical properties of miniature specimens on the plates.

The diagonal elements of the evaluated second order fiber orientation tensor are shown in Fig. 4 together with their cumulative distribution functions. The fiber orientation tensor is evaluated with the coordinate system shown in Fig. 1. The a_{11} component coincides with the 0° specimen direction. As the diagonal elements of the second order fiber orientation tensor sum up to 1, the a_{33} direction, the out of plane direction, is not shown, as it has the lowest values. Most fibers are oriented in a_{11} direction for both plates. However, next to the sprue, in the bottom rows, the a_{11} component is lower and the a_{22} component is higher. The cumulative distribution functions show a low difference between the two plates: The a_{11} component of the 90° plate is higher than that of the 0° plate.

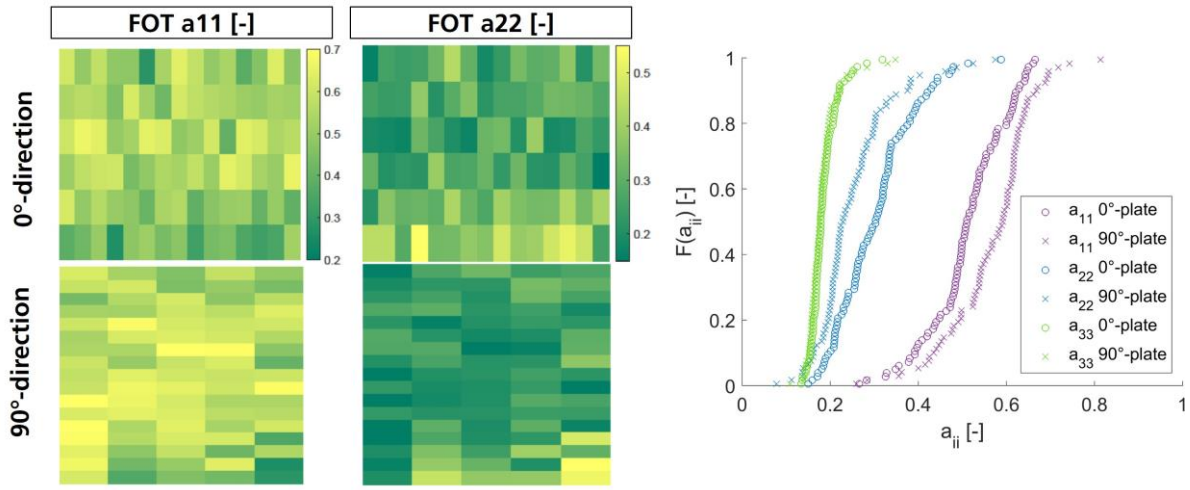

Figure 4: Local fiber orientation tensor.

The polished specimen heads show a high local scatter of the fiber orientation. Fig. 5 shows two different microscope images taken from the same specimen head. The microscope images have a distance of 3.2 mm. Although the microscope images are taken from the same specimen head, the fiber orientation shows a large variation. The right microscope image shows more fibers aligned in a_{11} direction that the left one.

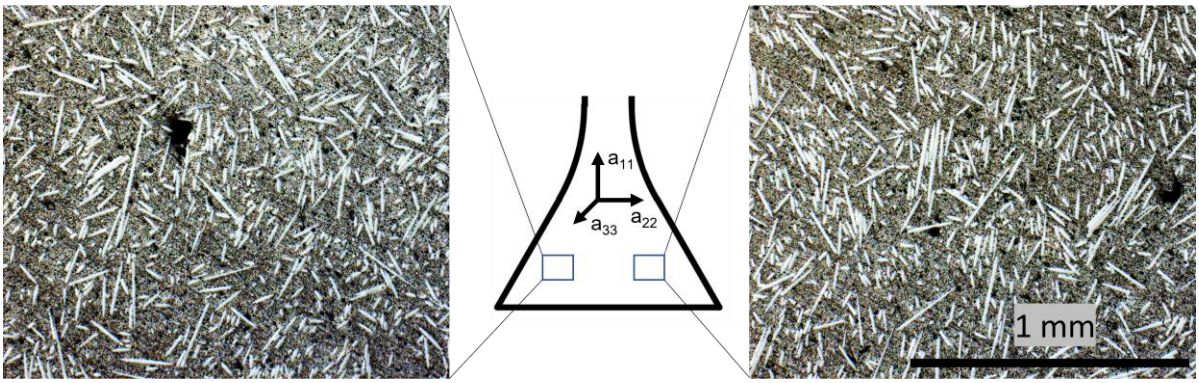

Figure 5: Two different evaluation images from the same specimen head from the middle of the 0° half plate.

The correlation of the mechanical properties and the fiber orientation are shown for both plates in Table 1. For both plates and testing directions exists a high positive correlation between the tensile strength and the fracture strain. If a specimen breaks at low strength, it also has a low fracture strain. For the 0° plate, there is a middle positive correlation between the Young's modulus and the tensile strength. For the 90° plate, there is a middle negative correlation between the Young's modulus and the fracture strain. For the 0° plate , the highest positive correlation between the fiber orientation and the mechanical properties is found for the Young's modulus and the a_{11} component of the FOT, which coincides with the negative correlation to the a_{22} component, as the a_{11} and the a_{22} component of the FOT are strongly negatively correlated.

For both plates, there is a slight positive correlation between the tensile strength and the specimen direction: for the 0° plate, R_m and a_{11} correlate slightly and for the 90° plate, R_m and a_{22}. With more fibers oriented in tensile direction, the tensile strength gets higher.

For both plates, there is likewise a slight positive correlation between the fracture strain and the component of the FOT transverse to the specimen direction: for the 0° plate, A and a_{22} correlate slightly and for the 90° plate, A and a_{11}.

0°\90°	FOT a_{22}	FOT a_{11}	E	R_m	A
FOT a_{22}	1.00	-0.93	0.08	0.12	-0.01
FOT a_{11}	-0.94	1.00	-0.08	0.00	0.09
E	-0.39	0.35	1.00	0.03	-0.37
R_m	-0.09	0.15	0.33	1.00	0.86
A	0.13	-0.04	-0.10	0.86	1.00

Table 1: Correlation matrix for 0°-specimens in lower triangle and 90°-specimens in upper triangle.

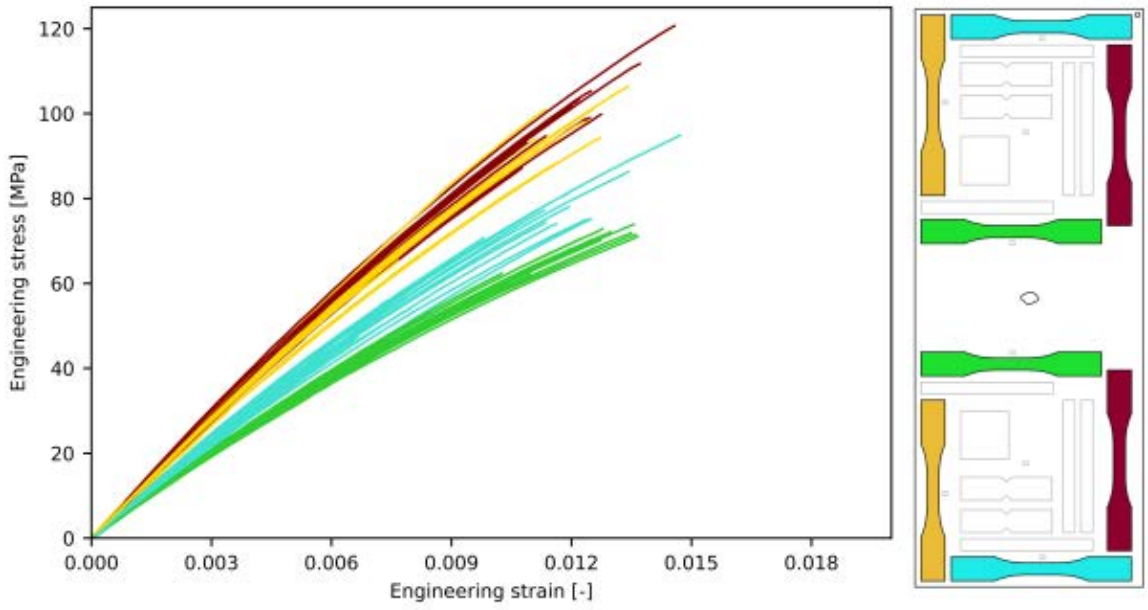

Figure 6: Stress-strain curves of ISO specimens with specimen plan in the same colors.

3.2 ISO size specimens

The stress-strain curves of the ISO specimens are shown together with their removal positions in Fig. 6. The curves of the four removal positions are differently colored. All tests show again a brittle fracture behavior without a visible necking of the specimen or a localization of the strains. The tensile strength and Young's modulus are likewise higher in 0° direction. The Young's modulus of the 90° specimens is next to the sprue lower than at the end of the plates. There is a scatter between the test curves of specimens taken from different plates at the same positions. However, this scatter is smaller than the difference between curves of specimens from different positions.

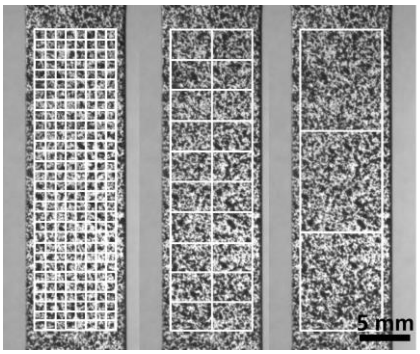

Figure 7: Different evaluation grids of local strain.

Additionally to the global strain evaluation, the strain in the tests of the ISO specimens is also evaluated locally. The local strain is evaluated for three different grid sizes shown in Fig. 7: a 30x8 grid with an edge length of 1 mm, a 10x2 grid and a 3x1 grid. The cumulative distribution functions of the local longitudinal, transverse and shear strain are shown in Fig. 8 for two exemplary specimens at a global longitudinal strain of 1%. For specimen 1, the local

properties show lower scatter for a larger grid. For specimen 2, especially the longitudinal strain and the shear strain show no grid size dependent behavior. This specimen has larger regions where the strains are similar in magnitude.

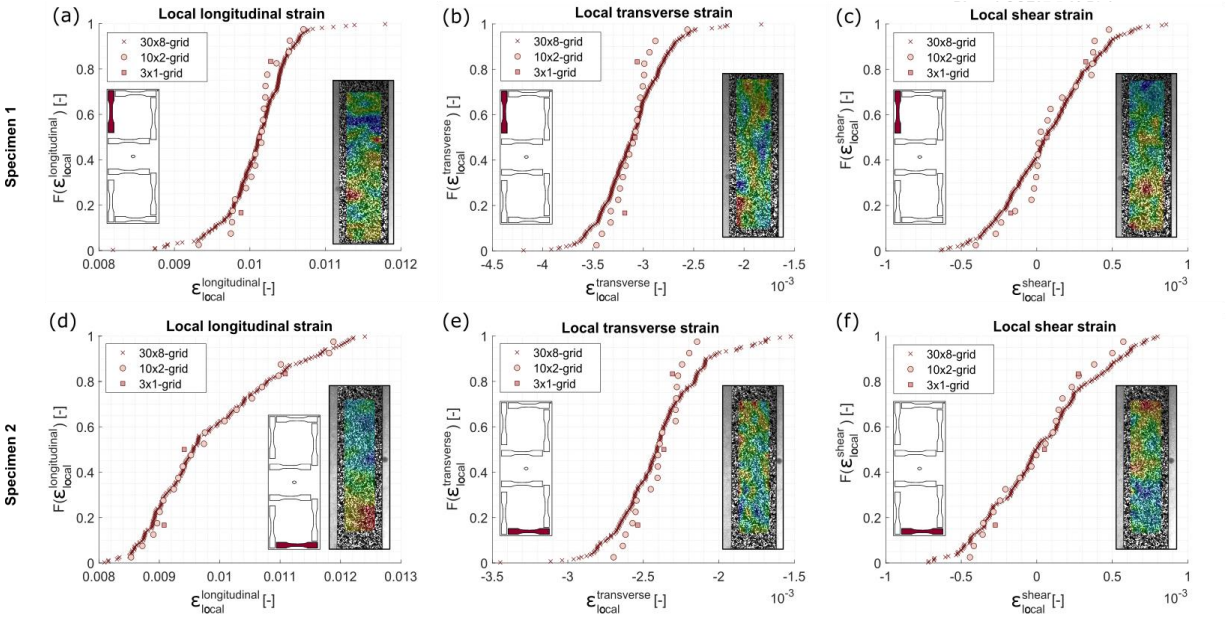

Figure 8: Local strain variation for two different specimens at global longitudinal strain of 1%. Shown are the cumulative distribution functions for the local longitudinal, transverse and shear strains for different sizes of evaluation grids.

3.3 Comparison of different specimen sizes

The two different tested specimen scales can be compared concerning their scatter. Therefore, the mechanical properties of tests on the two different investigated specimen sizes are given in Fig. 9. The cumulative distribution functions of the different specimens and testing directions and specimen positions are given for the Young's modulus, tensile strength and fracture strain. Additionally, the mean values and standard deviations of the mechanical properties are given in Table 2. The scatter of the mechanical properties is for the tests on the miniature specimens larger than for the tests on the ISO specimens. As the miniature specimens are taken from positions over the whole plate, their properties show the scatter on the whole plate. The scatter of the properties of the ISO specimens is the scatter between specimens taken from the same position of different plates. This means the scatter between different plates under the same manufacturing conditions is lower than the scatter inside a plate.

The Young's modulus and tensile strength values are for both specimen scales higher in 0° than in 90° because more fibers are aligned in 0°. The tensile strength values of the tests on the ISO specimens are in the upper range of the scatter of the tests on the miniature specimens for both directions. Perhaps the miniature specimens have a pre-damage because of the water-jet cutting process, which leads to a lower tensile strength. Or the higher surface-to-volume ratio of the miniature specimens leads to an earlier damage. The fracture strain of the tests on the ISO specimens is in both directions similar to the tests on the miniature specimens in 90°. The fracture strain of the tests on the 0° miniature specimens is slightly below the fracture strain of the other specimens.

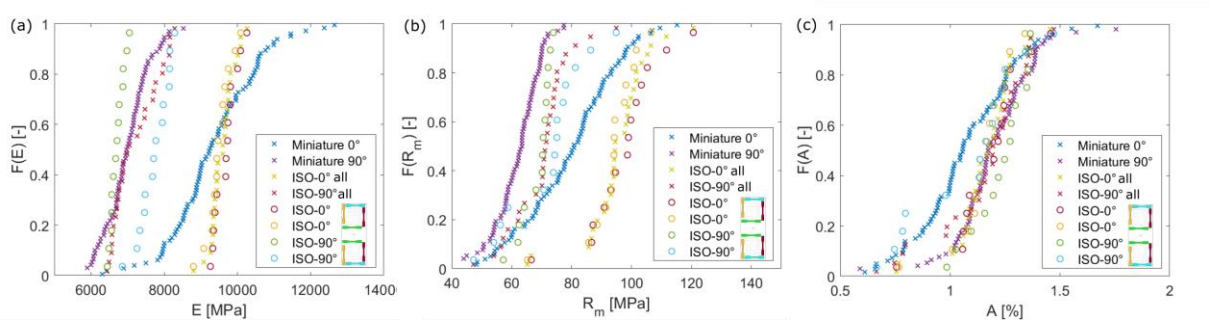

Figure 9: Mechanical properties of miniature and ISO size specimens as cumulative distribution functions: (a) Young's modulus, (b) tensile strength and (c) fracture strain.

	Miniature specimens		ISO size specimens	
	0°	**90°**	**0°**	**90°**
Young's modulus *E* [MPa]	9349 ± 12.9%	6909 ± 12.2%	9587 ± 3.4%	7219 ± 8.4%
Tensile strength R_m [MPa]	79 ± 20.2%	61 ± 18.6%	95 ± 11.8%	70 ± 14.2%
Fracture strain *A* [%]	1.07 ± 21.4%	1.19 ± 20.7%	1.16 ± 13.1%	1.15 ± 17.8%

Table 2: Material properties (mean values with standard deviations).

4 DISCUSSION AND SUMMARY

The investigated plates, coming all from the same manufacturing campaign, show direction dependent properties with a higher Young's modulus and tensile strength in 0°. In addition, the fiber orientation exhibits a high underlying scatter, which can vary greatly even within small areas. The scatter of the mechanical properties between the same position of different plates is lower than the scatter over an entire plate.

The investigated fiber-reinforced polymer, manufactured by an injection molding process, shows a flow dependent behavior of the mechanical properties superimposed by a high local scatter coming from a scatter of the fiber orientation. The large number of performed tests serves as an experimental data basis for a multiscale simulation approach. Similar to [9] for foams or [10] for sheet molding compound, the process-induced uncertainties of a short fiber-reinforced polymer can be investigated. The mechanical properties of the polymer matrix and the fiber-matrix interface are necessary for microstructure simulations in a multiscale simulation approach. The matrix properties can be determined from tensile tests on neat resin specimens. The fiber-matrix interface properties can be determined by single-fiber push-out tests [11][12] or micro tensile tests [13] on the composite material.

ACKNOWLEDGEMENTS

The authors thank Robert Maertens at the Fraunhofer Institute for Chemical Technology ICT in Pfinztal, Germany for the compounding of the thermoset molding materials and the injection molding of the specimen plates.

The present work has been funded by the Deutsche Forschungsgemeinschaft (DFG, German Research Foundation) under Grant no. 464119659. The financial support is gratefully acknowledged.

REFERENCES

[1] Maertens, R., Liebig, W.V., Elsner, P. and Weidenmann, K.A., *Compounding of Short Fiber Reinforced Phenolic Resin by Using Specific Mechanical Energy Input as a Process Control Parameter*, J. Compos. Sci., 5, **127**, 2021.

[2] Keyser, H. de, Berg, L.-F. and Stammler, J., *Composite materials ready to replace aluminium in internal combustion engines*, JEC Compos, **53**, 32-35, 2016.

[3] Englich, S., *Strukturbildung bei der Verarbeitung von glasfasergefüllten Phenolformaldehydharzformmassen*, PhD thesis, Universität Chemnitz, Chemnitz, Germany, 2015.

[4] Friedrich, J. and Michaeli, W., *Handbuch Spritzgiessen*, Hanser, Munic, Germany, 2002.

[5] Höer, M., *Einfluss der Material- und Verarbeitungseigenschaften von Phenolharzformmassen auf die Qualität spritzgegossener Bauteile*, PhD thesis, Universität Chemnitz, Chemnitz, Germany 2014.

[6] Phelps, J.H., Abd El-Rahman, A.I., Kunc, V. and Tucker, C.L., *A model for fiber length attrition in injection-molded long-fiber composites*, Compos Part A Appl Sci Manuf, **51**, 11-21, 2013.

[7] DIN EN ISO 527-4, *Determination of tensile properties – Part 4: Test conditions for isotropic and orthotropic fibre-reinforced plastic composites*, Beuth Verlag, Berlin, Germany, 1997.

[8] Advani, S.G. and Tucker, C.L., *The Use of Tensors to Describe and Predict Fiber Orientation in Short Fiber Composites*, J Rheol, **31**, 8, 751–784, 1987.

[9] Beckmann, C., and Hohe, J., *Numerical Prediction of Disorder Effects in Solid Foams using a Probabilistic Homogenization Scheme*, Mech Mat **78**, 22-43, 2014.

[10] Meyer, N., Gajek, S., Görthofer, J., Hrymak, A., Kärger, L., Henning, F., Schneider, M. and Böhlke, T., *A probabilistic virtual process chain to quantify process-induced uncertainties in Sheet Molding Compounds*, Compos B Eng, **249**, 110380, 2023.

[11] Jäger, J., Sause, M., Burkert, F., Moosburger-Will, J., Greisel, M., and Horn, S., *Influence of plastic deformation on single-fiber push-out tests of carbon fiber reinforced epoxy resin,* Compos Part A Appl Sci Manuf, **71**, 157–167, 2015.

[12] Rohrmüller, B., Gumbsch, P. and Hohe, J., *Calibrating a fiber-matrix interface failure model to single fiber push-out tests and numerical simulations*, Compos Part A Appl Sci Manuf, **150,** 106607, 2021.

[13] Fliegener, S., Kennerknecht, T., and Kabel, M., *Investigations into the damage mechanisms of glass fiber reinforced polypropylene based on micro specimens and precise models of their microstructure*. Compos B Eng, **112**, 327–343, 2017.